Thin Solid Films 520 (2012) 2173–2177

Contents lists available at SciVerse ScienceDirect

Thin Solid Films

journal homepage: www.elsevier.com/locate/tsf

High frequency magnetic behavior through the magnetoimpedance effect in CoFeB/(Ta, Ag, Cu) multilayered ferromagnetic thin films

M.S. Marques [a], T.J.A. Mori [b], L.F. Schelp [b], C. Chesman [a], F. Bohn [a], M.A. Corrêa [a,*]

[a] Departamento de Física Teórica e Experimental, Universidade Federal do Rio Grande do Norte, 59072-970 Natal, RN, Brazil
[b] Departamento de Física, Universidade Federal de Santa Maria, 97105-900 Santa Maria, RS, Brazil

ARTICLE INFO

Article history:
Received 3 May 2011
Received in revised form 11 October 2011
Accepted 14 October 2011
Available online 20 October 2011

Keywords:
Magnetic films and multilayers
Anisotropy
Magnetic measurements
Magnetoimpedance effect
Sputtering

ABSTRACT

We investigate the structural and magnetic properties and the magnetoimpedance effect of CoFeB/(Ta, Ag, Cu) multilayered thin films grown by magnetron sputtering. It is noticed that the peak of maximum magnetoimpedance ratio values for a given frequency, as well as its position in frequency, is varied according to the used non-magnetic metal. For the CoFeB/Ta and CoFeB/Ag multilayered films, peaks of 30% and 27%, respectively, are observed at localized frequency ranges. For the CoFeB/Cu multilayer, slightly smaller values are verified, but for a wide frequency range. The magnetoimpedance results are analyzed in terms of the mechanisms responsible for the impedance variations at different frequency ranges and the magnetic and structural properties of the multilayer.

1. Introduction

The magnetoimpedance effect (MI) has attracted considerable interest in recent times mainly due to its potential application in high-performance sensors and sensing elements in integrated circuits, which can be used in a wide variety of sectors, such as biology and geo-studies [1,2].

MI corresponds to the change in complex impedance $Z = R + iX$ of a ferromagnetic sample submitted to an external magnetic field H. In general, the impedance changes with the magnetic field, at different frequency ranges, are interpreted in terms of three distinct mechanisms. At low frequency values, up to MHz decades where the skin effect is weak, impedance changes are associated to variations in its inductive part (L), an effect known as magnetoinductance [3]. At intermediate frequencies, from decades of MHz to hundreds of MHz, the main mechanism is the skin effect, where a change in transverse magnetic permeability is observed. However, at high frequency values, from hundreds of MHz to GHz, although the skin effect is still observed, the field configuration inside the sample usually induces ferromagnetic resonance (FMR) effect, the main mechanism responsible for changes in magnetic permeability and MI, since domain wall motion is strongly damped by eddy currents. However, even from this traditional point of view, the precise limits between the frequency ranges are strongly dependent on magnetic anisotropy and, particularly, on the dimensions and geometry of the sample.

The effect has been studied extensively in samples such as ribbons [4–6] and microwires [7–9]; however, more recently, an increasing interest have been devoted to the MI of single and multilayered thin films [10–19], which present interesting magnetic and structural properties, that can be used, for example, in integrated devices sensors.

In the specific case of thin films, samples of F/NM multilayer, where F is a ferromagnetic alloy and NM is a non-magnetic metallic material, generally have excellent properties for the study of the MI. Among the properties which stand out are high magnetic permeability, high values for saturation magnetization, low relaxation parameter values (α) and high electrical conductivity.

With this spirit, for some years now, our group has carried out researches on different ferromagnetic alloys for the growth of multilayer [15,16,19], such as Permalloy ($Ni_{81}Fe_{19}$), with saturation magnetization $M_S \sim 780$ kA/m [20] and magnetostriction constant $\lambda \sim 10^{-8}$ [20], and the amorphous precursor of the nanocrystalline Finemet ($Fe_{73.5}Cu_1Nb_3Si_{13.5}B_9$), $M_S \sim 1030$ kA/m [21] and $\lambda \sim +20 \times 10^{-6}$ [22].

In this article, we study a CoFeB ferromagnetic alloy, with $M_S \sim 625$ kA/m [23] and $\lambda \sim +10^{-6}$ [24]. As a motivation to use this alloy, CoFeB alloys have great technological potential, being used, e.g., in microwave absorbers [25], shielding materials [26], strain gauges [24] and magnetic random access memories (MRAMs) [27]. Thus, here, we investigate the structural and magnetic properties and the MI in F/NM multilayer, where F is a CoFeB alloy, and NM are Ta, Ag or Cu. In particular, the MI results are discussed in terms of structural and magnetic characteristics of the samples and of the mechanisms responsible by the impedance variations at different frequency ranges.

* Corresponding author. Tel.: +55 84 36068089; fax: +55 84 32119217.
E-mail address: marciocorrea@dfte.ufrn.br (M.A. Corrêa).

0040-6090/$ – see front matter © 2011 Elsevier B.V. All rights reserved.
doi:10.1016/j.tsf.2011.10.028

2. Experiment

In this study, we produced a series of multilayer ($Co_{40}Fe_{40}B_{20}$/(NM))×50, where NM = Ta, Ag or Cu), grown using the magnetron sputtering technique. The samples were deposited onto glass substrates, covered by a Ta buffer layer, and finally covered again by a Ta cap layer. Fig. 1 shows the structure of the samples deposited. In these samples, deposition time was necessary to obtain the nominal thickness of the 9 nm ferromagnetic layers, 2 nm non-magnetic layers, and 5 nm buffer and cap layers. The deposition process was carried out with the following parameters: base pressure of 6×10^{-6} Pa, Ar pressure during deposition of 2.66×10^{-1} Pa, 90 W RF power supply for the CoFeB alloy and a DC current of 25 mA for the Ta, Ag or Cu metallic layers. Using these parameters, deposition rates were 0.33 nm/s for $Co_{40}Fe_{40}B_{20}$ and 0.18 nm/s, 0.91 nm/s and 0.29 nm/s for Ta, Ag and Cu, respectively.

In order to induce magnetic anisotropy and define an easy magnetization axis, the substrates were submitted to a 80 kA/m magnetic field inside the chamber during deposition. Fig. 1 shows the direction of the magnetic field, indicated by the arrow, applied transversely to the main axis of the sample. Magnetic properties were obtained using an alternate gradient field magnetometer, at room temperature, with a maximum magnetic field of ±24 kA/m, in two directions: along the direction defined by the field applied during deposition (EA), and perpendicular to this direction (HA).

The structural properties of the multilayered thin films were obtained from measurements of X-ray reflectivity (XRR). The diffractograms were acquired at small angles θ from 0.25° to 5.00°, using a Bruker AXS D8 Advance diffractometer, and Bragg–Brentano geometry (θ–2θ) with Göbel mirrors at the outlet of the tube in order to make the beam parallel. For a detailed review on this topic, we suggest Refs. [28,29]. Besides, in order to obtain further information, such as the layers' thickness and interfaces' roughness of each sample, we performed experimental data fittings and simulations using the "Software for modeling the optical properties of multilayered films — IMD", whose methods and calculations are outlined in detail in [30].

The impedance $Z(f, H)$ measurements were performed as a function of field and frequency using an HP4396B spectrum-impedance-network analyzer equipped with an HP43961A impedance test kit and an appropriate microwave cavity. In this case, the sample is the central stripe conductor, which is separated from the ground plane by the glass substrate. The probe current was fed directly to one side of the sample, while the other side was in short circuit with the ground plane. In this case the current flows along the sample length. To the impedance measurements, samples were cut to a size of 3×10 mm^2, with the main axis in HA direction, and fixed to microstripline sample holder using silver glue, where all contacts were made with 24 h cured low resistance silver paint. All measurements were performed in as-cast deposited samples. The MI measurements were performed varying the magnetic field in small steps between ±24 kA/m over a wide frequency range, from 10 MHz to 1.8 GHz. For all measurements, while the external magnetic field was swept, a 0 dBm (1 mW) constant power was applied to the sample, characterizing a linear regime of driving signal. At a given field value, the frequency sweep was made and the real and imaginary parts of the line impedance were simultaneously acquired. For further information on this procedure, we suggest Refs. [17,31]. The curves presented hysteretic behavior, associated with coercive field. However, in order to clarify the general behavior, just curves when the field goes from the negative to the positive values are presented. From the measurements, the MI ratio was defined as

$$MI\% = \frac{Z(H) - Z(H_{max})}{Z(H_{max})}, \quad (1)$$

where $Z(H)$ is the impedance value at a given field H and $Z(H_{max})$ is the impedance at the maximum applied magnetic field H_{max}, where the magnetic state of the sample is saturated. Finally, MI_{max} is defined as the maximum $MI\%$ value for a given frequency.

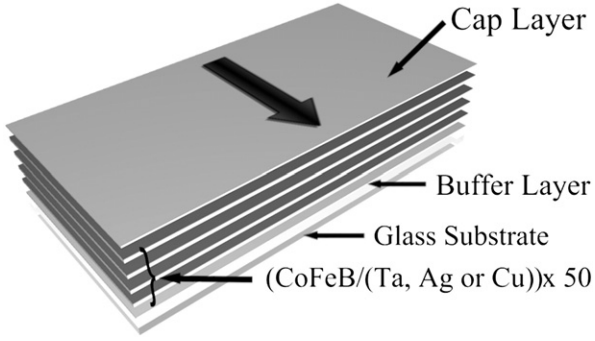

Fig. 1. Schematic structure of the multilayer. The sample consists of a multilayer, formed by 50 bilayers of CoFeB/NM, where NM are Ta, Ag or Cu are deposited onto a glass substrate covered by a Ta buffer layer and, finally, covered by a Ta cap layer. The larger arrow indicates the direction of the magnetic field applied during sample deposition, transversely to the main axis of the sample.

3. Results and discussion

3.1. Structural properties

The XRR measurements for CoFeB/Ta, CoFeB/Ag and CoFeB/Cu can be found in Fig. 2. All the three samples present chemical modulation perpendicular to the substrate. However, from the decreasing of the relative intensity of successive Bragg peaks, it is clear that the multilayered films have quite different morphologies. This is confirmed by the simulations and fittings made from models, that are also shown for all spectra in Fig. 2 (red solid lines). They reproduce well the main features of the experimental data, specially with we consider the large number of bilayers. The quality of the multilayer (i.e. layer thickness, homogeneity and interface flatness) depends substantially on the difference in surface free energy between the materials included in the structure. When Ta is used as magnetic material spacer, this difference is small and the growth mode leads to layers with almost constant thickness and flat interfaces. This can be seen in Table 1, that shows the parameters used in each simulation. The CoFeB/Ta multilayer presents roughnesses of the order of one monoatomic layer, very close to an ideal sample. Ag and Cu, on the other hand, are immiscible with Co and Fe and tend to have very different surface-free energies from that of the magnetic material. This prevents the complete wetting of the surfaces when one material is deposited over the other, and generates layers with less homogeneous thickness and rougher interfaces. Both CoFeB/Cu and CoFeB/Ag samples present this characteristic, but with an important difference:

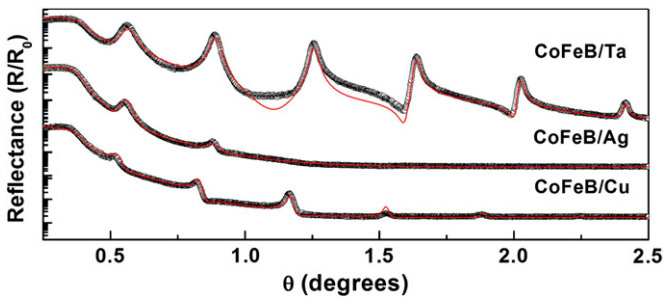

Fig. 2. XRR experimental patterns (black empty circles) for our multilayer films, together with the experimental data fittings/simulations (red solid lines). The main parameters obtained through the XRR experimental data fitting for each multilayer thin film are presented in Table 1.

Table 1
Main parameters obtained through the XRR experimental data fitting and used for simulations for each multilayer: ferromagnetic layer thickness, non-magnetic metallic material layer thickness, and roughness of the interfaces between the layers.

Sample parameters	CoFeB/Ta	CoFeB/Ag	CoFeB/Cu
CoFeB thickness (nm)	9.15	9.15	9.15
NM thickness (nm)	2.00	2.00	2.83
CoFeB/NM roughness (nm)	0.15	3.16	4.00
NM/CoFeB roughness (nm)	0.00	2.03	0.50

when Ag is used as a NM spacer, the fluctuations in the layer thickness (roughness) are large and almost symmetrically distributed over the successive interfaces. In the case of Cu, the roughness is large in the CoFeB/Cu but small at the Cu/CoFeB interfaces. This asymmetry arises from differences in the growing mode when the staking sequence is changed. When CoFeB is deposited over Cu, the atoms mobility leads to the formation and nucleation of CoFeB islands, whose topology appears as roughness in the CoFeB layer surface, i.e., layer thickness fluctuations. When Cu atoms arrive at a rough CoFeB surface, they produce a smooth interface and tend to decrease the roughness by filling the voids and valley of the CoFeB surface. This behavior has been identified and addressed in detail for Co over Cu and Cu over Co [32]. Despite the differences in the composition and cristallinity, it seems to be followed also here. If we take into account the roughness of CoFeB/Cu and Cu/CoFeB interfaces and the Cu thickness, it is possible that the correct staking is destroyed in certain regions of this sample. As we will see in the following sections, this picture is consistent with the quasi-static magnetic behavior.

3.2. Quasi-static magnetic properties

The magnetic properties of the multilayered thin films were measured through magnetization curves obtained from a magnetic field oriented along and transversal to the direction of the magnetic field applied during deposition. Fig. 3 shows the magnetization curves measured for our set of samples.

By comparing these curves, it is possible to verify the magnetic anisotropy induced during film growth for the CoFeB/Ta and CoFeB/Ag samples, confirming the easy magnetization axis EA oriented transversely to the main axis of the sample and along the same direction of the magnetic field applied during deposition. In these cases, saturation fields are approximately 5.57 kA/m and 3.66 kA/m for CoFeB/Ta and CoFeB/Ag samples, respectively.

On the other hand, in the CoFeB/Cu sample, we perceived weak anisotropy induction and an increase in the coercive field when compared to results for CoFeB/Ta and CoFeB/Ag samples. In particular, this fact can be associated with the non-formation of regular bilayers in the CoFeB/Cu multilayer, as previously discussed. The formation of islands instead of continuous layers results in an increase in structural disorder and subsequent storage of higher internal stress as the sample is grown; this gives rise to random local-field anisotropies which result in weak effective anisotropy oriented in the direction of the magnetic field applied during deposition.

As effective anisotropy directly influences the dynamic results of magnetization, the MI measurements of these multilayered films reflect exactly the differences discussed.

3.3. MI results

Fig. 4 shows impedance Z as a function of both magnetic field and frequency for the CoFeB/Ta, CoFeB/Ag and CoFeB/Cu samples (left side), together with Z curves as a function of the magnetic field for selected frequency values (right side). While all the impedance measurements in this study were obtained from a wide range of frequency levels (10 MHz to 1.8 GHz), a very low signal-to-noise ratio was recorded for frequencies up to ~300 MHz. This result is related to the low thickness of the multilayer grown and the subsequent appearance of the skin effect only at higher frequency levels. For this reason, Z behavior is only shown for frequencies of 500 MHz or higher. Besides, taking into account the main mechanisms responsible by the MI variations, already discussed in Section 1, it must be pointed out that, due to sample geometry and frequency range considered, just the skin and FMR effects can be observed.

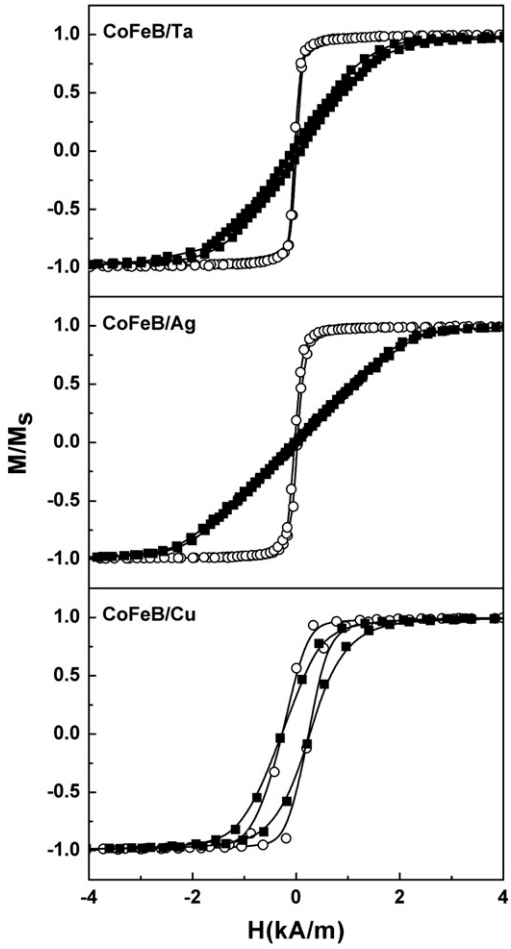

Fig. 3. Magnetization curves for the CoFeB/Ta, CoFeB/Ag and CoFeB/Cu samples, obtained when the magnetic field is applied along (open circles) and transversely (closed squares) to the direction defined by the magnetic field applied during the deposition, i. e., perpendicularly to the main axis of the sample.

For the whole frequency range, all samples exhibit similar behavior, characterized by a double peak structure. For the CoFeB/Ta and CoFeB/Ag multilayered films, this feature is associated to the fact that the magnetic field and the current are transversally applied to the easy magnetization axis [4]. In particular, Fig. 4 shows that in the CoFeB/Ta sample, maximum Z position remains stable up to a frequency of ~990 MHz, while in the CoFeB/Ag sample, the change in Z peak position occurs at frequencies higher than ~1.19 GHz. This result indicates that the behavior of both samples is very similar. Nonetheless, the most striking result can be seen for the CoFeB/Cu sample, where a displacement in Z peaks was observed at much lower frequency levels, from ~450 MHz. In this case, for this sample which presents weak magnetic anisotropy, the double peak behavior is connected to appearance of the FMR effect contribution.

In all samples, along the entire frequency band in which Z peak position remains stable, the main mechanism responsible for MI behavior is the skin effect. On the other hand, the change in Z peak position in accordance with magnetic field as frequency increases reflects the fact that FMR effect becomes the main mechanism

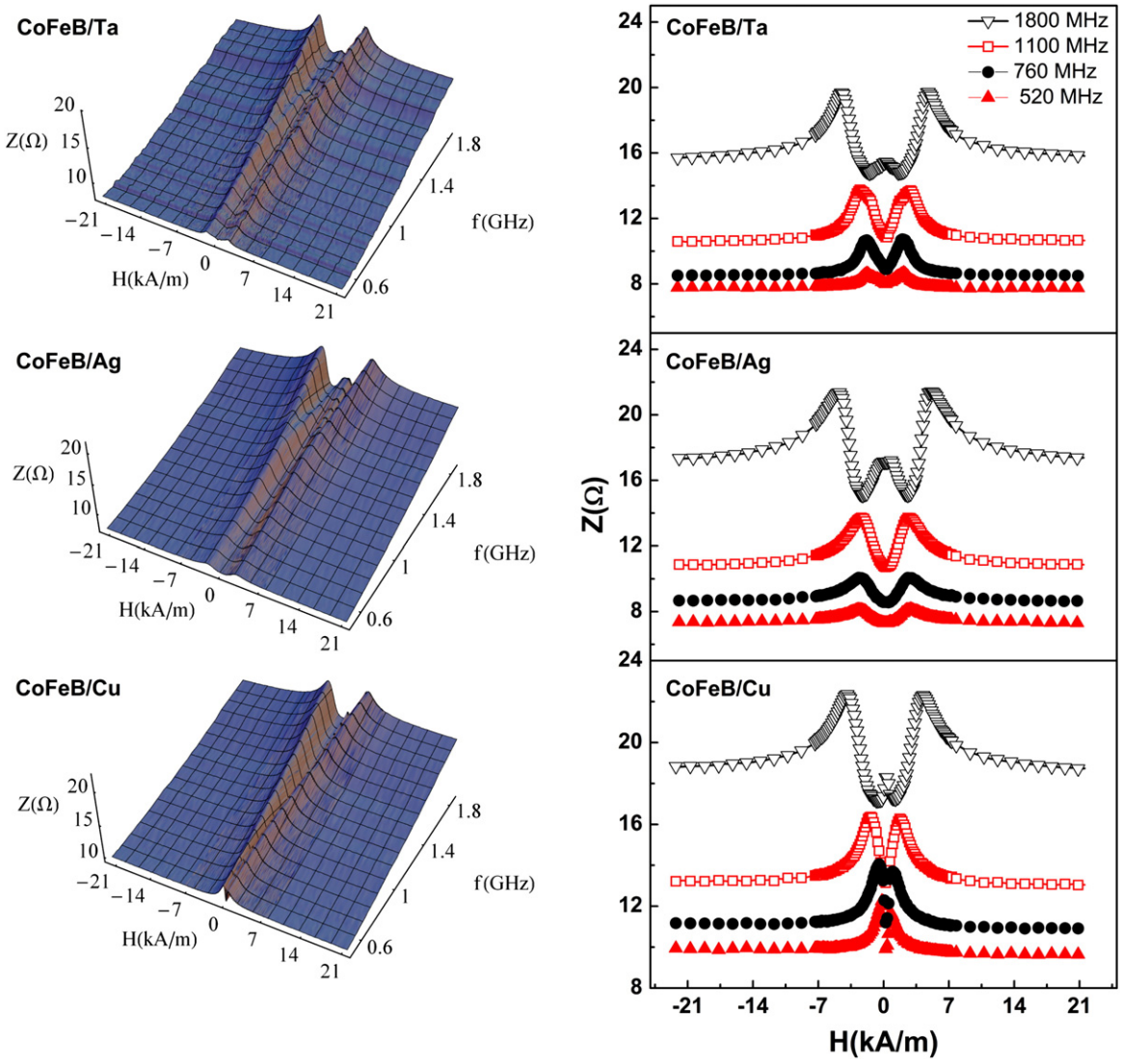

Fig. 4. Impedance Z as a function of the magnetic field and frequency for the CoFeB/Ta (top), CoFeB/Ag (middle) and CoFeB/Cu (bottom) samples. Left side: The complete set of Z curves are presented as a function of both H and f, showing the general magnetic behavior of the multilayered thin films. Right side: In order to guide the eyes, Z curves as a function of the magnetic field for selected frequency values. All the Z curves exhibit hysteretic behavior; however, to clarify the general behavior, only the curves obtained when the field goes from the negative to the maximum positive values are presented.

responsible for variations in impedance. The contribution of the FMR effect to Z was verified using the method described by Barandiarán et al. [33], and previously employed by our group in [19]. In this case, in the CoFeB/Ta and CoFeB/Ag samples, the contribution of FMR effect to MI behavior was observed at frequency levels starting at ~760 MHz and ~950 MHz, respectively. In the CoFeB/Cu sample, a small contribution of FMR to the MI was observed starting already at frequency levels of ~420 MHz. This behavior at a lower frequency level may be associated with the presence of random local anisotropies induced by stress. Therewith, in this sample, the weak magnetic anisotropy favors the appearance of localized resonances, contributing to MI variation starting at lower frequency levels.

As a final point, Fig. 5 shows MI_{max} vs. f behavior obtained from measurements of impedance in the multilayered films. For the CoFeB/Ta, a single peak reaching MI_{max} of around 30% is verified close to 1 GHz, while for the CoFeB/Ag, variations of 27% at a frequency level of 1.25 GHz is observed. This behavior is similar to those obtained by our group in multilayered films produced with other compositions [15,16,19]. The same figure also presents the influence of the FMR effect in the CoFeB/Cu sample. In this case, the distribution of stress-induced anisotropies and the non-formation regular bilayers results in smaller impedance variations of around 25%. However, these variations occur for a wide range of frequencies, frequencies from 600 MHz to 1 GHz.

Thus, this framework qualifies samples with distinct anisotropies for different technological applications. While samples with well-

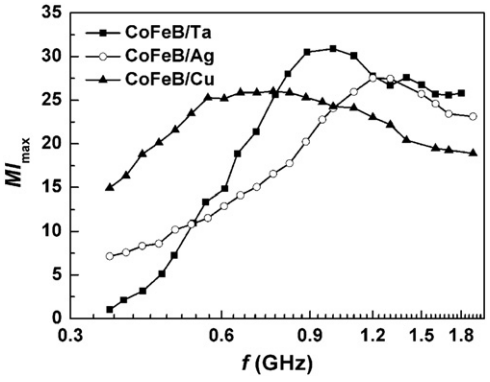

Fig. 5. MI_{max} versus f for the CoFeB/Ta, CoFeB/Ag and CoFeB/Cu samples.

defined anisotropies are characterized by greater impedance variations within a narrow frequency band and can be used in devices requiring good MI response at localized frequency, samples with weakly induced anisotropies, when used as sensor elements, are able to provide impedance variations which, albeit lower, is almost linear even with frequency variations in the excitation circuit during use.

4. Conclusion

In this article, we presented a study of the structural and magnetic properties and the MI of CoFeB/(Ta, Ag, Cu) multilayer. The structural properties obtained from measurements of XRR in the CoFeB/Ta and CoFeB/Ag samples were characterized by good bilayer uniformity when compared to those of the CoFeB/Cu sample, whose structure consists of CoFeB layers interspersed with Cu islands. Such structural properties influenced the magnetization behavior, as can be verified through the effective anisotropies observed in the magnetization curves. The mechanisms responsible for greater variations in MI occur at high frequencies associated with the emergence of FMR effect in the CoFeB/Ta and CoFeB/Ag samples. On the other hand, in the CoFeB/Cu sample, due to the formation of islands in the Cu layer and the weak induction of effective anisotropy resulting from localized anisotropies oriented in different directions, we observed the contributions of FMR at much lower frequency levels than in the other multilayered films. Here, we confirmed variations of up to 30% in the CoFeB/Ta sample at a frequency level of 1 GHz, and variations of 27% at a frequency level of 1.25 GHz in the CoFeB/Ag sample. Finally, the CoFeB/Cu sample, in particular, demonstrated behavior relevant to the use of sensor elements requiring constant variations in the MI within a wide frequency range. In this sample, we noted an efficiency level of approximately 25%, obtained, however, within a wide range of frequencies, from 600 MHz to 1 GHz.

With these results and the ones previously published by our group [15,16,19], we end a cycle of studies related to the MI in multilayered thin films with different ferromagnetic alloys. In Ref. [19], we studied the MI in magnetic multilayer of NiFe/Ag with different geometries and it was observed MI_{max} of about 80%, at ~1 GHz. On the other hand, Refs. [16,17], we presented a comparison between samples of the amorphous precursor of the Finemet with distinct geometries (single layer, multilayer and sandwich thin films), where it was verified MI_{max} of about 250%, at ~1.2 GHz, for the multilayered one.

So, what lessons can be drawn from our results? First, according the choice of the ferromagnetic alloy, which presents specific structural and magnetic properties, it is possible to tune the largest value of MI_{max} to a given frequency, if the sample presents a defined magnetic anisotropy, or a slightly smaller value of MI_{max} to a wide range of frequency, if the one has weak magnetic anisotropy. Second, with respect to the sample geometry, by employing multilayer samples with defined magnetic anisotropy, it is possible to tune just one frequency where MI_{max} present high values [15,16]. By using multilayer with the sandwich geometry, for example, it is possible to obtain two tuned frequencies where the MI_{max} present high values [19]. Consequently, the optimal response for technological applications, such as magnetic sensors and integrated devices based on the magnetoimpedance effect, is defined by two choices: the first is related to the ferromagnetic alloy, while the second one is associated to the sample geometry. These two choices taken together will lead to the characteristic behavior of the element sensor.

Acknowledgments

The research was partially supported by the Brazilian agencies by CNPq (No. 476429/2010-2), CAPES, FAPERJ, FAPERGS and FAPERN. M. A.C. and F.B. acknowledge financial support of the INCT of Space Studies.

References

[1] Z.M. Wu, K. Huang, S.P. Li, J.Y. Kang, Z.J. Zhao, X.L. Yang, Sens. Actuators, A 161 (2010) 62.
[2] R. Valenzuela, J.J. Freijo, A. Salcedo, M. Vázquez, A. Hernando, J. Appl. Phys. 81 (1997) 4301.
[3] K. Mohri, T. Kohsawa, K. Kawashima, H. Yoshida, L.V. Panina, IEEE Trans. Magn. 28 (1992) 3150.
[4] R.L. Sommere, C.L. Chien, Phys. Rev. B 53 (1995) 5982.
[5] A.D. Santos, L.G.C. Melo, C.S. Martins, F.P. Missell, Y. Souche, F.L.A. Machado, S.M. Rezende, J. Appl. Phys. 79 (1996) 6546.
[6] K.R. Pirota, L. Kraus, M. Knobel, P.G. Pagliuso, C. Rettori, Phys. Rev. B 60 (1999) 6685.
[7] J. Valázquez, M. Vázquez, D.X. Chen, A. Hernando, Phys. Rev. B 50 (1994) 16737.
[8] K. Mohri, L.V. Panina, T. Uchiyama, K. Bushida, M. Noda, IEEE Trans. Magn. 31 (1995) 1266.
[9] D.P. Makhnovskiy, L.V. Panina, D.J. Mapps, Appl. Phys. Lett. 77 (2000) 121.
[10] R.L. Sommer, C.L. Chien, Appl. Phys. Lett. 67 (1995) 3346.
[11] T. Morikawa, Y. Nishibe, H. Yamadera, Y. Nonomura, M. Takeuchi, Y. Taga, IEEE Trans. Mag. 33 (1997) 4367.
[12] S.-Q. Xiao, Y.-H. Liu, S.-S. Yan, Y.-Y. Dai, L. Zhang, L.-M. Mei, Phys. Rev. B 61 (2000) 5734.
[13] G.V. Kurlyandskaya, J.L. Muñoz, J.M. Barandiarán, A. García-Arribas, A.V. Svalov, V. O. Vas'kovskiy, J. Magn. Magn. Mater. 242 (2002) 291.
[14] F. Amalou, M.A.M. Gijs, Appl. Phys. Lett. 81 (2002) 1654.
[15] M.A. Corrêa, A.D.C. Viegas, R.B. da Silva, A.M.H. de Andrade, R.L. Sommer, Physica B 384 (2006) 162.
[16] M.A. Corrêa, A.D.C. Viegas, R.B. da Silva, A.M.H. de Andrade, R.L. Sommer, J. Appl. Phys. 101 (2007) 043905(1)-043905(6).
[17] M.A. Corrêa, F. Bohn, A.D.C. Viegas, A.M.H. de Andrade, L.F. Schelp, R.L. Sommer, J. Phys. D: Appl. Phys. 41 (2008) 175003(1)-175003(6).
[18] R.B. Silva, A.D.C. Viegas, V.P. Nascimento, M.A. Corrêa, L.F. Schelp, E. Baggio-Saitovitch, R.L. Sommer, Appl. Phys. Lett. 94 (2009) 042501(1)-042501(3).
[19] M.A. Corrêa, F. Bohn, C. Chesman, R.B. da Silva, A.D.C. Viegas, R.L. Sommer, J. Phys. D: Appl. Phys. 43 (2010) 295004(1)-295004 (7).
[20] B.D. Cullity, Introduction to Magnetic Materials, Addison-Wesley, New York, 1972.
[21] R. Hasegawa, J. Magn. Magn. Mater. 304 (2006) 187.
[22] V.H. Duong, R. Grössinger, R.S. Turtelli, C. Polak, J. Magn. Magn. Mater. 157/158 (1996) 193.
[23] H. Naganuma, M. Oogane, Y. Ando, J. Appl. Phys. 109 (2011) 07D736(1)-07D736 (3).
[24] D. Wang, C. Nordman, Z. Qian, J.M. Daughton, J. Myers, J. Appl. Phys. 97 (2005) 10C906(1)-10C906(3).
[25] X. Shen, H.-F. Li, H.-H. Li, J.-H. Nie, J. Mater. Sci. - Mater. Electron. 20 (2009) 272.
[26] J.-J. Jiang, Q. Ma, S.-W. Bie, G. Du, B. Tian, Z.-K. Feng, H.-H. He, Trans. Nonferrous Met. Soc. China 17 (2007) s725.
[27] J.M. Teixeira, R.F.A. Silva, J. Ventura, A.M. Pereira, F. Carpinteiro, J.P. Araújo, J.B. Sousa, S. Cardoso, R. Ferreira, P.P. Freitas, Mater. Sci. Eng., B 126 (2006) 180.
[28] H.P. Klug, L.E. Alexander, X-ray Diffraction Procedures: For Polycrystalline and Amorphous Materials, Wiley-Interscience, Nova York, 1974.
[29] B.D. Cullity, Elements of x-ray Diffraction, Addison-Wesley, Reading, 1978.
[30] D.L. Windt, Comput. Phys. 12 (1998) 360.
[31] A.D.C. Viegas, M.A. Corrêa, L. Santi, R.B. da Silva, F. Bohn, M. Carara, R.L. Sommer, J. Appl. Phys. 101 (2007) 033908(1)-033908(7).
[32] T.J. Minvielle, R.L. White, R.J. Wilson, J. Appl. Phys. 79 (1996) 5116.
[33] J.M. Barandiarán, A. García-Arribas, D. de Cos, J. Appl. Phys. 99 (2006) 103904(1)-103904(4).